

621.01(06)

W. Piekarska, M. Kubiak

Czestochowa University of Technology, Poland

Tel. +48 (034) 325 06 99; E-mail: piekarska@imipkm.pcz.pl**ISSUES IN NUMERICAL MODELLING OF THERMAL PHENOMENA
ACCOMPANYING MODERN WELDING TECHNOLOGY**

This work contains issues of mathematical and numerical modelling of thermal phenomena in welding process using two modern welding methods: laser beam welding and advanced laser-arc hybrid welding technology. Modelling of temperature field with the motion of liquid metal in the fusion zone taken into account is presented. Coupled heat transfer and fluid flow phenomena are described. Latent heat associated with material's state changes is considered in heat transfer solution algorithm. Using elaborated models, results of calculations were obtained including temperature field and melted material velocity field in the fusion zone of butt-welded joints. Implemented in ObjectPascal programming language computer solver was used in order to solve complex numerical modelling issues.

Keywords: thermal phenomena, laser beam welding, hybrid welding, numerical modelling.

Introduction

The need for increasingly better quality and performance of welded joints has contributed to the development of new welding methods. The implementation of modern technologies such as laser beam welding and hybrid welding is often a breakthrough in many industries, enabling the production of innovative constructions [1]. It is possible to make various joints of different kinds of materials using the laser beam with or without additional material [2].

Highly concentrated laser beam causes very rapid material melting, which allows for a very high welding speed with a small amount of molten material and a small heat affected zone (HAZ). In recent years there has been a significant growth in the use of a laser beam in different types of welded joints. Lasers are for example used in robotic welding of car body parts in the automotive industry or ship construction parts.

However, the need for a precise set-up of welded elements and hardening of welded joints (in HAZ or weld itself) in some cases limit its application, especially when joining elements with a significant thickness. Therefore, alternative methods are constantly looked for. Recently, attention is paid to hybrid welding technology. Laser-arc hybrid welding is a method combining two welding techniques - laser beam with classical electric arc welding [3].

An important feature of laser beam as a high power and concentration heat source is the deep penetration of welded material. This penetration depth, which results from the process analysis [1, 4] is closely related to the heat source power density and concentration as well as physical properties of the material. The local increase in temperature leads not only to melting, but also to the local evaporation and creation of the "keyhole", which is also a heat source penetrating welded material [4, 5]. Hybrid welding process combines deep material penetration by a laser beam with a good gap filling in electric arc welding process.

Heat transfer and convective motion of a liquid material in the welding pool determine the geometry of the weld. The effect of metal heating during welding depends on the distribution and amount of heat introduced through two heat sources into welded material.

Therefore, an important step in the modeling of thermal phenomena in welding is the selection of appropriate heat sources parameters.

Computational analysis of thermal phenomena in welding processes is quite complicated. Often requires special numerical procedures for determining certain thermal phenomena or the introduction of specific boundary conditions [6, 7]. Papers describing mathematical modeling and numerical simulation of laser welding process appear in the literature for many years [4, 5, 8]. Whereas most of research concerning laser-arc hybrid welding process are focused on the experimental study about effective way to combine two welding methods in a single process [2, 3]. Numerical models, which appear in the last few years, are based mainly on the solutions used in the modeling of autonomous laser welding and electric arc welding [9-11].

An appropriate estimation of temperature distribution in the joint is the essential issue during modeling of thermal phenomena because temperature determines the shape and size of the weld and HAZ. Correctly determined temperature field and characteristic zones of the joint allows to specify microstructure composition and properties of welded construction [7, 8, 12].

This work contains mathematical and numerical modelling of temperature field taking into account the motion of a liquid metal in the melted zone in advanced welding techniques using a laser beam, that is single laser beam welding and laser-arc hybrid welding. Coupled heat transfer and fluid flow in the melted zone phenomena are described respectively by heat transfer equation with convective term and Navier-Stokes equation with natural convection and flow through porous medium in the mushy zone (Fig. 1). The numerical solution algorithm takes into account the latent heat associated with material's state changes.

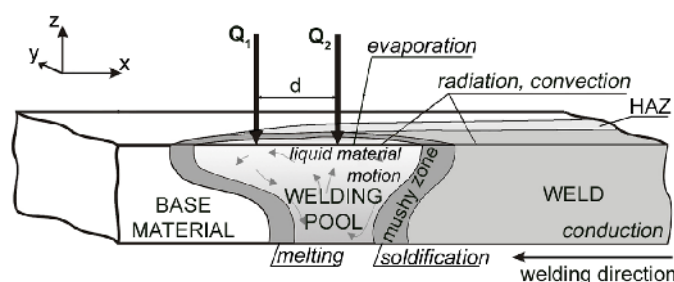


Fig. 1. Considered phenomena in laser-arc hybrid welding process

Results of calculations including temperature field and melted material velocity field in butt-welded joints are presented in this study. Numerical solutions of governing differential equations were performed using projection method and finite volume method (FVM) [13]. On the basis of elaborated numerical models computer solver was developed. The solution algorithm was implemented in ObjectPascal programming language.

Heat sources

In laser beam welding depth of penetration of laser radiation in metal is about 10-4 - 10-5 cm. Absorbed laser light vaporise material and forms a “keyhole” that contains ionised vapour. The laser power is absorbed in the ionised vapour and transferred to the walls of the “keyhole” forming the weld pool. A very important issue, taking into account the formal rules of numerical modelling, is the selection of an appropriate heat source model used in calculations. The new mathematical models of the distribution of energy flux delivered to

the material and further transport of the energy into the material are constantly looked for in order to represent the real welding conditions as much as possible. In the number of papers published in recent years attention is paid to the numerical models of heat sources in the laser heating process. The papers mostly apply to a surface heat source models, but there are much less studies focused on the numerical models of welding heat sources (taking into consideration the laser beam penetration depth) [4, 5].

Essentially the Gaussian distribution model is used to describe the laser beam heat source power distribution, in the following form:

$$Q_s(r) = \frac{fQ}{\pi r_0^2} \exp\left(-f \frac{r^2}{r_0^2}\right), \quad (1)$$

where Q is the laser beam power [W], r_0 is the beam radius [m], $r = \sqrt{x^2 + y^2}$ is the current radius [m] and coefficient f (usually assumed as $f=3$) characterizes the beam distribution.

The mechanism of material melting by a laser beam is usually recognized as a volumetric heat source model. In analytical and analytical-numerical considerations, shape of the source is adopted in the form of equivalent volume of a cylinder of given radius r_0 and height d , assuming a constant beam power over the entire laser beam penetration depth

$$Q_v(r, z) = \frac{Q}{\pi r_0^2 d} \exp\left(-\frac{r^2}{r_0^2}\right) u(z), \quad (2)$$

where $u(z) = 1$ for $0 \leq z \leq d$ and $u(z) = 0$ for other positions of z , z is a current depth.

Volumetric heat sources in the shape of a cone or truncated cone with linear decrease of energy density along laser beam penetration deep in the material are often found in the literature [4, 5, 10]. Laser beam power distribution close to real conditions is obtained using cylindrical-involution-normal (C-I-N) [5] model, described by the following equation:

$$Q_v(r, z) = \frac{kK_z Q}{\pi(1 - e^{-(K_z s)})} e^{-(kr^2 + K_z z)} [1 - u(z - s)], \quad (3)$$

where $K_z = 3/s$ is the heat source power exponent [m^{-1}], $k = 3/r_0^2$ is the beam focus coefficient [m^{-2}] and s is heat source beam penetration depth [m], $u(z - s)$ is the Heaviside's function.

This heat source model, by changing s , k and K_z parameters, allows for modelling of variety concentrated heat source shapes with exponential decrease of heat source energy with material penetration depth. Depending on s factor the "keyhole" can be considered as a paraboloid when workpiece thickness is grater or equal s or truncated paraboloid when s is grater than the thickness (Fig. 2).

The most appropriate model for electric arc heat source is a 'double ellipsoidal' Goldak's heat source model [14]. This widely accepted by the researchers heat source distribution can be used to simulate various arc parameters and has very good features of power density distribution control in the weld and heat affected zone.

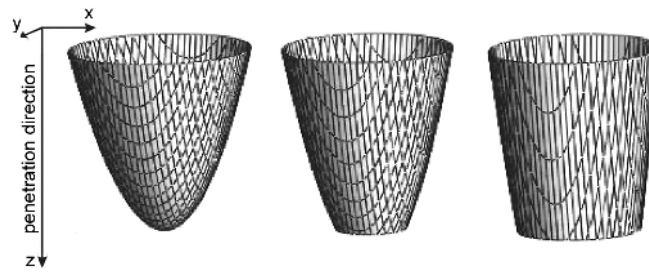


Fig. 2. Shapes of CIN volumetric heat source

The shape of Goldak's heat source is a combination of two half-ellipses connected to each other with one semi-axis (Fig. 3), defined as follows:

$$Q_v = \begin{cases} q_1(x, y, z) = \frac{6\sqrt{3}f_1Q}{abc_1\pi\sqrt{\pi}} \exp(-3\frac{x^2}{a^2}) \exp(-3\frac{y^2}{b^2}) \exp(-3\frac{z^2}{c_1^2}) \\ q_2(x, y, z) = \frac{6\sqrt{3}f_2Q}{abc_2\pi\sqrt{\pi}} \exp(-3\frac{x^2}{a^2}) \exp(-3\frac{y^2}{b^2}) \exp(-3\frac{z^2}{c_2^2}) \end{cases}, \quad (4)$$

where a , b , c_1 and c_2 are set of axes that define front ellipsoid and rear ellipsoid, f_1 and f_2 ($f_1 + f_2 = 2$) represent distribution of the heat source energy at the front and the rear section, thus resultant distribution of the source energy is total sum described as $q_v(x, y, z) = q_1(x, y, z) + q_2(x, y, z)$, $Q = UI$ is the heat source power [W], U is voltage [V], I is arc current [A].

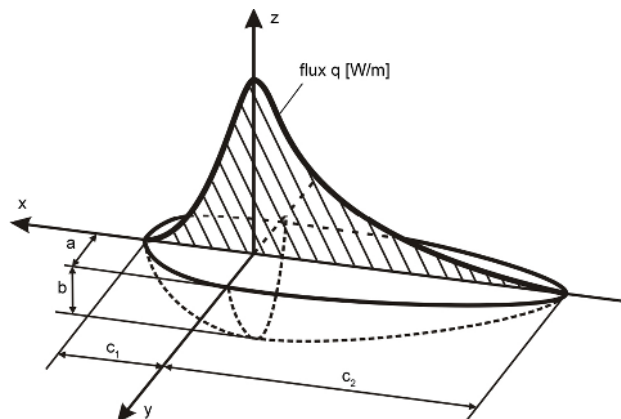


Fig. 3. Shape of Goldak's double ellipsoidal volumetric heat source

Technological parameters of hybrid welding process, such as relative arrangement of laser beam and electric arc, distance between two heat sources as well as electric arc and laser beam power should be correctly set to obtain narrow weld with highest possible quality of the join. In numerical analysis hybrid heat source power distribution is used as a product of Goldak's (4) and CIN (3) heat sources.

Temperature field

Temperature field depends mainly on the welding speed and distribution of heat energy delivered by welding heat sources. Natural convection of liquid material in the fusion zone plays also important role as well as latent heat associated with material's state changes during melting, solidification and evaporation phenomena. The temperature field is obtained by the solution of transient heat transfer equation with convective term, expressed as follows:

$$\frac{\partial}{\partial x_i} \left(\lambda \frac{\partial T}{\partial x_i} \right) = C_{ef} \left(\frac{\partial T}{\partial t} + v_i \frac{\partial T}{\partial x_i} \right) - \tilde{Q}, \quad (5)$$

where $T=T(x_i, t)$ is a temperature at a point x_i , v_i is a velocity vector, $\lambda=\lambda(T)$ is a thermal conductivity, $C_{ef}=C_{ef}(T)$ is an effective heat capacity which includes latent heat associated with material's state change, \tilde{Q} is a volumetric heat source with laser beam and electric arc power distributions taken into considerations.

Initial condition: $t = 0 : T = T_0$ and boundary conditions complete equation (5), taking into account a heat loss due to convection, radiation and evaporation

$$\Gamma : -\lambda \frac{\partial T}{\partial n} = \alpha(T|_{\Gamma} - T_0) + \varepsilon \sigma (T^4|_{\Gamma} - T_0^4) - q_o + q_v, \quad (6)$$

where α is convective coefficient, ε is radiation coefficient, and σ is Stefan-Boltzmann constant. Element q_o is the heat flux towards the top surface of the welded element ($z=0$) in the source activity field, while q_v represents heat loss due to material evaporation in area where $T \geq T_L$, Γ is a boundary of analysed domain.

Phase transformations due to material's state changes are considered in effective heat capacity C_{ef} . Below solidus temperature C_{ef} is a product of density and specific heat in solid state. Between solidus and liquidus temperatures, the latent heat of fusion is included into the effective heat capacity [8-10], with assumed linear approximation of porosity coefficient.

$$C_{ef}(T) = \rho_{SL} c_{SL} + \rho_S \frac{H_L}{T_L - T_S} \text{ for } T \in [T_S; T_L], \quad (7)$$

where T_S and T_L are solidus and liquidus temperatures respectively, H_L is a latent heat of fusion, $c_{SL} \rho_{SL} = c_S \rho_S (1 - f_l) + c_L \rho_L (f_l)$ is the product of density and specific heat in the mushy zone.

Between liquidus temperature and boiling point of steel the effective heat capacity is a product of density and specific heat in liquid state. Assuming a linear approximation of a liquid phase $f_{l-g} \in [0; 1]$ between the boiling point and maximum temperature, and assuming full equilibrium of metal evaporation pressure in the "keyhole" and shielding gases pressure, the effective heat capacity in temperatures exceeding boiling point is defined as follows:

$$C_{ef}(T) = \rho_L c_L + \frac{\rho_L H_b}{T_{max} - T_b} \text{ for } T \geq T_b, \quad (8)$$

where T_b is a boiling point of steel, T_{max} is a maximum temperature, H_b is a latent heat of evaporation.

Liquid material flow through the welding pool

Liquid material flow in the fusion zone considered in the computational model allows for an analysis of previously neglected phenomena associated with the dynamics of welding pool formation [9] and affects calculated temperature distribution in welded element, in consequence having significant influence on numerically estimated geometry of the weld and heat affected zone [10].

Velocity field of a liquid material in the melted zone is obtained by the solution of Navier–Stokes equations fulfilling the continuity equation with buoyancy forces and flow through the porous medium taken into consideration.

$$\frac{\partial \rho}{\partial t} + \frac{\partial}{\partial x_i}(\rho v_i) = 0, \quad (9)$$

$$\frac{\partial(\rho v_i)}{\partial t} + \frac{\partial}{\partial x_j}(\rho v_i v_j) = -\frac{\partial p}{\partial x_i} + \frac{\partial}{\partial x_j} \left(\mu \frac{\partial v_i}{\partial x_j} \right) + \rho \beta_T (T - T_{ref}) - \frac{\mu}{K} v_i, \quad (10)$$

where ρ is a density, \mathbf{g} is acceleration of gravity, β_T is a volume expansion coefficient due to heating, T_{ref} is a reference temperature, μ is a dynamic viscosity, K is porous medium permeability.

Equation (10) is completed by initial condition $t = 0: \mathbf{v} = 0$ and boundary conditions implemented at the welding pool boundary determined by solidus temperature ($T_{ref} = T_s$), which are described as follows:

$$\Gamma: \mathbf{v}|_{\Gamma} = 0, \quad \tau_s = \mu \frac{\partial \mathbf{v}}{\partial n} = \frac{\partial \gamma}{\partial T} \frac{\partial T}{\partial s}, \quad (11)$$

where τ_s is Marangoni shear stress in the direction tangent to the surface, γ is surface tension coefficient.

Porous medium permeability K in the mushy zone is described by Carman–Kozeny equation [9]

$$K = K_0 \frac{f_l^3}{(1 - f_l)^2}; \quad K_0 = \frac{d_0^2}{180}, \quad (12)$$

where f_l is porosity coefficient, d_0 is an average solid particle diameter.

Numerical solutions

Differential equations describing thermal phenomena in discussed welding processes are numerically solved using projection method with FVM. The spatial variables are discretized using a staggered grid to avoid odd-even decoupling between the pressure and velocity. Velocity components are calculated at nodal points placed in the middle of each control volume face, while the pressure, density and temperature are calculated at the centre of control volume (Fig. 4).

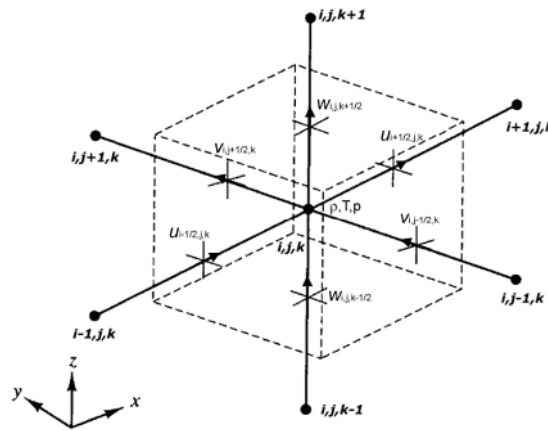


Fig. 4. Elementary control volume in a staggered grid

In the first step of projection, equation (10) is solved without momentum changes due to pressure forces

$$\frac{\mathbf{v}^* - \mathbf{v}^s}{\Delta t} = -\nabla \cdot (\mathbf{v}\mathbf{v})^s + \frac{1}{\rho^s} \left(\mu \nabla^2 \mathbf{v}^s + \rho^s \mathbf{g} \beta_T (T - T_{ref}) - \frac{\mu}{K} \mathbf{v}^s \right), \quad (13)$$

In the second step, the projection of temporary velocity \mathbf{v}^* onto \mathbf{v}^{s+1} is made according to the following formula:

$$\frac{\mathbf{v}^{s+1} - \mathbf{v}^*}{\Delta t} = -\frac{1}{\rho^s} (\nabla p^{s+1}), \quad (14)$$

The formula (14) with the continuity equation (9) is combined into one Poisson equation

$$\nabla \cdot \left(\frac{1}{\rho^s} (\nabla p^{s+1}) \right) = \frac{1}{\Delta t} \nabla \cdot \mathbf{v}^*, \quad (15)$$

In every time step Poisson equation (15) is solved by BiCGStab method [15] with Jacobi preconditioner to find the pressure, at which the velocity at the new time step is divergence free.

Because forward Euler integration scheme is used in calculations as well as central difference quotients, quality of the results depends on the conditions of stability. Time step constraints and additional stabilization methods for high Peclet numbers [13] are taken into account in solution algorithms to ensure proper quality of results.

Examples of computer simulations

On the basis of described solution methods computer solver was created allowing 3D numerical simulations of thermal phenomena accompanying laser beam welding and laser-arc hybrid welding processes. Laser beam technological parameters were set to: welding speed $v=1.2$ m/min, laser beam power $Q_L=3800$ W, laser beam radius $r_0=1$ mm and penetration deep $s=5$ mm, laser efficiency $\eta_L=85\%$. The simulation of laser-arc hybrid welding process

was performed in geometrical set-up with leading electric arc in the tandem. Parameters of additional electric arc heat source were set to: arc current $I=310\text{A}$, welding voltage $U=31.8\text{V}$, arc efficiency $\eta_A=75\%$. Distance between arc torch and laser beam focal point was set to $d=5\text{mm}$ and welding speed $v=2.6\text{ m/min}$. The dimensions of the butt welded steel sheets were set to $150\times30\times4\text{mm}$.

Fig. 5 presents results of laser beam and hybrid welding computer simulations, including temperature field at the top surface and in longitudinal section of welded sheets, with melted steel velocity field in. Solid line (solidus isotherm) determines the shape and size of welding pool. Temperature field and melted material velocity field in the cross section of the joint are illustrated in Fig. 6 with additionally marked (dashed line) boundary of heat affected zone ($T_g\ 1000\text{K}$).

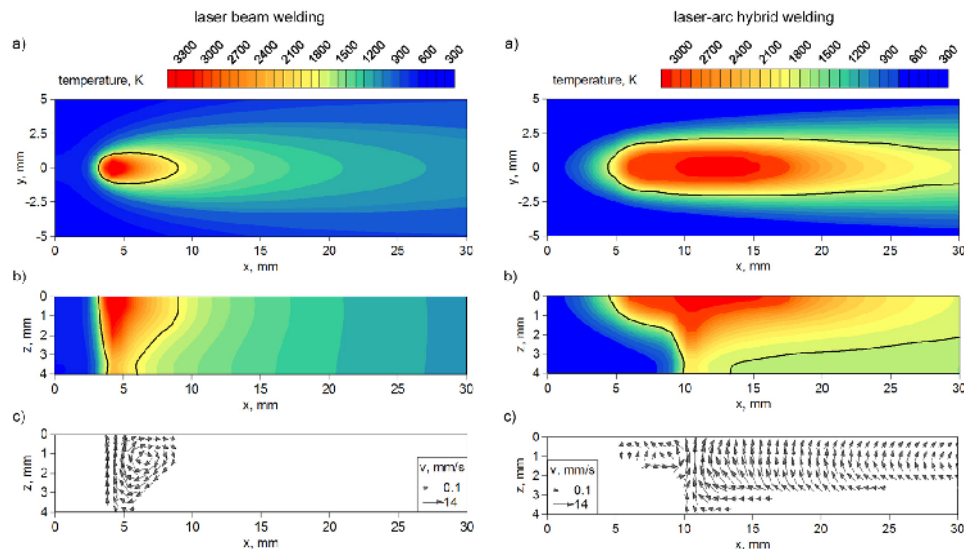


Fig. 5. Temperature field a) at the top surface of welded sheet and b) in longitudinal section of the weld with c) melted material velocity field

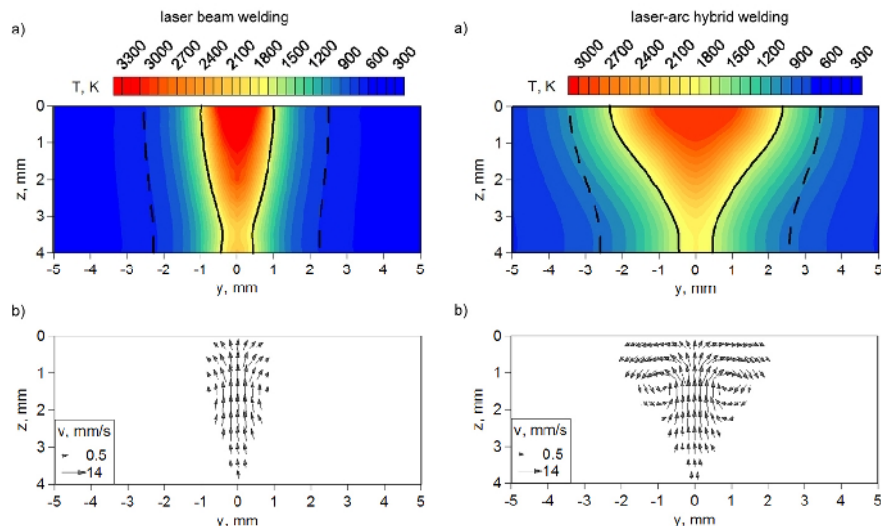


Fig. 6. Cross section of welded joints, a) temperature field and b) melted material velocity field in the fusion zone

Conclusions

Numerical modelling of thermal phenomena in modern welding technology is quite complicated, due to the fact that material melting and weld formation takes place in different conditions in comparison to conventional welding methods. Therefore, numerical analysis of thermal phenomena requires a slightly different modelling approach than the classical welding.

Perfect contact of butt welded sheets and welding without additional material is assumed in numerical analysis. Comparison of obtained temperature field and melted material velocity field during simulation of single laser beam welding and laser-arc hybrid welding processes shows that the use of hybrid heat source significantly changes material melting process.

As shown in longitudinal section of welded joint (Fig. 5b) electric arc in hybrid welding melts upper parts of the workpiece, which allows for a better material penetration by the laser beam, therefore a higher welding speed can be used in this process in comparison to single laser beam welding.

Obtained temperature field in the cross-section of the weld (Fig. 6) allows for determination of the weld and heat affected zone geometry. It is observed that motion of melted material in the welding pool has a significant influence on the weld shape, especially in the hybrid welding process.

References:

1. Dawes C. Laser Welding: A practical guide / Dawes C. – New York: Abington Publishing, 1992. – 261 p.
2. Technological applications of laser beam welding and cutting at the Instytut Spawalnictwa / Pilarczyk J., Banasik M., Dworak J. et al. – Warszawa: Przegląd Spawalnictwa, 2006. – Vol. 5-6. – 6-10 p.
3. Bagger C. Review of laser hybrid welding / Bagger C., Olsen F.O. // Laser Institute of America: Journal of Laser Applications, 2005. – Vol. 17. – 2-14 p.
4. Gery D. Effects of welding speed, energy input and heat source distribution on temperature variations in butt joint welding / Gery D., Long H., Maropoulos P. // Elsevier: Journal of Materials Processing Technology. – 2005. – Vol. 167. – 393-401 p.
5. Ranatowski E. Thermal modelling of laser welding. Part I: The physical basis of laser welding / Ranatowski E. // Gdańsk Scientific Society: Advances in Materials Science. – 2003. – Vol. 1. – N. 3. – 34-40 p.
6. Makhnenko V.I. Role of mathematical modelling in solving problems of welding dissimilar steels (Review) / Makhnenko V.I., Saprykina G.Y. // E.O. Paton Institute: Paton Welding Journal. – 2002. – Vol. 3. – 14-25 p.
7. Numerical Methods for the Predictions of Welding Stresses and Distortions / Makhnenko V.I., Velikoivanenko E.A., Pochinok V.E. et al // Taylor & Francis: Welding and Surfacing Reviews, B.E. Paton (Ed.). – 1999. – Vol. 13. – N. 1. – 146 p.
8. Bokota A. Modeling of residual stresses in laser welding / Bokota A., Piekarska W. // E.O. Paton Institute: Paton Welding Journal. – 2008. – Vol. 6. – 19-24 p.
9. Cho J.H. Three-Dimensional analysis of molten pool in GMA-Laser hybrid welding / Cho J.H., Na S.J. // American Welding Society: Welding Journal. – 2009. – Vol. 88. – 35-43 p.
10. Piekarska W. Three-dimensional model for numerical analysis of thermal phenomena in laser-arc hybrid welding process / Piekarska W., Kubiak M. // Elsevier: International Journal of Heat and Mass Transfer. – 2011. – Vol. 54. – N. 23-24. – 4966-4974 p.

11. Kong F. Numerical and experimental study of thermally induced residual stress in the hybrid laser–GMA welding process / Kong F., Ma J., Kovacevic R. // Elsevier: Journal of Materials Processing Technology. – 2011. – Vol. 211. – 1102-1111 p.
12. Makhnenko V.I. Probabilistic characteristics of high-cycle fatigue resistance of structural steel welded joints / Makhnenko V.I. Romanova I.Yu. // E.O. Paton Institute: Paton Welding Journal. – 2010. – Vol. 7. – 7-11 p.
13. Patankar S.V. Numerical heat transfer and fluid flow / Patankar S.V. – USA: Taylor & Francis, 1990. – 197 p.
14. Goldak J.A. Computational Welding Mechanics / J.A. Goldak, M. Akhlaghi. – New York: Springer, 2005. – 323 p.
15. Van der Vorst, H.A. Bi-CGSTAB: A Fast and Smoothly Converging Variant of Bi-CG for the Solution of Nonsymmetric Linear Systems / Van der Vorst, H.A. // Society for Industrial and Applied Mathematics: SIAM Journal on Scientific and Statistical Computing. – 1992. – Vol. 13. – 631-644 p.

20.02.2012.

• , • • , •

:

—

.

—

,

.

•

,

•

,

•

•

,

ObjectPascal.

•

9

—

,

•

,

ObjectPascal.

•

3